



International Conference on Knowledge Based and Intelligent Information and Engineering Systems, KES2017, 6-8 September 2017, Marseille, France

## Texture analysis in watermarking paradigms

Margarita Favorskaya<sup>a\*</sup>, Anna Pyataeva<sup>b</sup>, Aleksei Popov<sup>a</sup>

<sup>a</sup>Siberian State Aerospace University, 31 Krasnoyarsky Rabochy ave., Krasnoyarsk, 660037 Russian Federation

<sup>b</sup>Siberian Federal University, 26, Kirensky st., Krasnoyarsk, 660074 Russian Federation

---

### Abstract

Digital watermarking algorithms have been developed rapidly as a response on the challenges caused by various internet attacks that are distorted the content of the host image and watermark partially or fully. In this paper, the issues of texture analysis with a goal to detect the most suitable image areas for embedding are discussed. The statistical and model-based methods are investigated as a trade-off between the computational cost and quality of the detected areas, where the embedded bits of a watermark could be the most invisible for a human vision. The criteria for detection of such areas based on the textural, contrast, illumination, and color coherence of the host image and watermark are formulated. The experiments show that the statistical methods based on the gradient oriented Local Binary Patterns (LBP) provide better computational time regarding to fractal estimation of textural image areas.

© 2017 The Authors. Published by Elsevier B.V.  
Peer-review under responsibility of KES International

*Keywords:* Local warping; video stabilization; motion level; keypoints; line segment; arc; interpolation

---

### 1. Introduction

Robust watermarking algorithms are the subject for investigation in last decades. The internet attacks against the image watermarking tools have become more sophisticated and diverse. Broadly, five types of solutions, such as spread spectrum modulation, invariant transform, template insertion, synchronization correction, and feature-based approach, have been addressed to solve these problems<sup>1</sup>. Each type mentioned above includes a wide family of the watermarking algorithms, which often need in the reasonable choice of areas for embedding. The preferable areas

---

\* Corresponding author. Tel.: +7-391-213-9623; fax: +7-391-291-9247.  
E-mail address: [favorskaya@sibsau.ru](mailto:favorskaya@sibsau.ru)

are the textural areas with the heterogeneity structure and corresponding scale. Therefore, the texture analysis is very useful function in digital watermarking. Methods for texture analysis can be categorized into six groups mentioned below:

- Structural methods describe the texture as a set of 2D texels (texture elements) using the mathematical morphology, keypoint detectors, or various descriptors<sup>2</sup>.
- Statistical methods study the spatial distribution of gray-levels in a given surrounding. The co-occurrences of gray-levels on circular neighborhoods<sup>3</sup> and in the path taken by the agent, when performing the walk<sup>4</sup>, provide the random projecting measurements of texture.
- Spectral methods simulate the texture in the power spectrum domain, for example using a bank of Gabor filters<sup>5</sup>.
- Model-based methods are based on the famous fractal geometry<sup>6</sup>, autoregressive models, Markov random fields, where images are modeled as the undirected graphs, among others.
- Recently appeared, agent-based methods consider the autonomous entity methods, e.g. random walks processes on graphs<sup>7</sup>.
- Graph-based methods represent an image as a graph, where each pixel is a vertex and the edges are generated regarding to the location and intensity of neighboring pixels, or the complex neural networks are applied for classification<sup>8</sup>.

Not all of these categories are suitable as a preliminary stage in the watermarking algorithms with the goal of perfect invisibility of a watermark. It is reasonable to investigate the statistical and model-based methods in order to detect the most gradient texture areas in a host image. The main idea of the statistical methods is to capture the spatial distribution of gray-levels and describe a texture in a compact form. The fractal methods calculate the fractal dimension or represent a texture description as a feature vector invariant to the bi-Lipschitz transformations in the multiscale fractal dimension<sup>9</sup>, multifractal spectrum<sup>6</sup>, and local fractal dimension<sup>10</sup>.

Our contribution deals with the deep analysis of methods for gradient evaluation of texture images and the matching of visual properties of the host image and watermark. The gradient evaluation of the textured areas in a host image is required for better frequency-based watermarking, while the matching of visual properties facilitates the invisibility of the watermarked host image. For gradient evaluation, the statistical and model-based approaches were applied and the comparative results were obtained.

This paper is organized as follows. Section 2 contains an overview of related work. The study of texture detection using the modified LBP and fractal estimations are discussed in Sections 3 and 4, respectively. Some recommendations for region choice in watermarking embedding are considered in Section 5. The comparative experimental results are represented in Section 6. Section 7 summarizes this study.

## 2. Related work

In this section, the most suitable approaches for texture analysis in the watermarking task are surveyed. One may concern to them the LBP methods (Section 2.1) and fractal methods (Section 2.2).

### 2.1. Overview of LBP modifications

During the past decades, many statistical methods, such as the co-occurrence matrix, wavelet transform, Gabor filter, Radon transform, and the LBPs, were developed and successfully tested using multiple texture datasets. The LBPs first introduced by Ojala et al.<sup>11</sup> are the useful, fast, and often applied technique for texture analysis. Despite the great success of the LBPs application in many tasks, the conventional LBP operator has the following drawbacks:

- The LBP produces long histograms, which are sensitive to image rotation.
- The LBP cannot detect large-scale textural structures because of its small surrounding.
- The LBP loses local textural information because the signs of pixels' differences are only obtained.
- The LBP is very sensitive to noise.

In order to overcome these problems, many modifications of the LBP operators were proposed by many researchers, for example the extended LBP<sup>12</sup>, where the concept of the uniform patterns were presented, the LBP with noise suppression using a binary decision function that accepts a special subset of LBPs called the texture primitives<sup>13</sup>, the Local Edge Patterns (LEPs) improving the gradient information<sup>14</sup>, the dominant local binary patterns<sup>15</sup>, etc. Some local patterns of textures are depicted in Fig. 1.

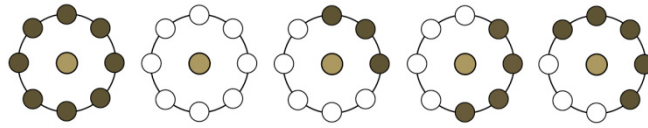


Fig. 1. different local patterns of textures from left to right: bright spot, dark spot, dark corner, edge, bright corner.

In some studies, the LBP enhanced the gradient calculation and edge detection in an image<sup>16</sup>, while in others the LBP was applied to the gradient magnitude images obtained by a Sobel operator<sup>17</sup>.

## 2.2. Overview of fractal methods

The concept of fractal was introduced by Mandelbrot and Van Ness<sup>18</sup>. Hereinafter, many algorithms have been proposed for systems with different physical properties including the texture analysis in 2D image<sup>19,20</sup>. A fractal set with a highly irregular structure but possesses a certain degree of self-similarity tends to fill the whole space and is appeared as a union of many ever smaller copies of itself. Such property is described by the Fractal Dimension (FD), which is based on the definition of Hausdorff measure in a view of the Hausdorff-Besicovitch dimension<sup>21</sup>. The complexity of computation of the Hausdorff-Besicovitch dimension led to many alternative definitions, such as the Box Counting Dimension (BCD), radius of gyration dimension, nested box dimension, and correlation function dimension. Li et al.<sup>22</sup> modified the BCD method by the selection of a box height that provides a finer measure for counting the box numbers, determination of a number of boxes that guarantees the least number of boxes, and completely covering an image surface by overlapping blocks. These procedures permitted to improve the estimate accuracy.

The multiscale fractal dimension based on the Bouligand–Minkowski fractal dimension can be applied to shape classification<sup>23</sup>. This dimension is estimated by the derivative of the fractality curve (minimum and maximum values, area under graph curve, etc.). Lazebnik et al.<sup>24</sup> proposed a fractal technique, which is based on a sophisticated point-based texture representation. The main idea was to characterize the texture by clusters of elliptic regions. Then the ellipses were transformed into circles such that a local descriptor became invariant to affine transform. Two descriptors, such as the spin image and rotation-invariant feature transform, were defined in each region. The resulting texture descriptor was a histogram of clusters of these local descriptors compared by the Earth mover's distance.

The term “multifractal spectra” was introduced in a sense to “restore” the dynamics, the phenomenon that can be called the multifractal rigidity<sup>25</sup>. Hereinafter, this concept was developed in some researches<sup>6</sup> called as the MultiFractal Spectrum (MFS) vector. The MFS is the general and globally invariant under the bi-Lipschitz transform and at the same time has low dimension, which is efficiently computed. Xu et al.<sup>26</sup> proposed the MFS estimation based on the low-, middle-, and high-frequency components in a wavelet pyramid. Such texture descriptor demonstrated the robustness to geometric transformation, global scale changes, and photometric variations (due to the MFS properties), better numerical stability, and efficient computation.

## 3. Local binary patterns for detection of textural areas

The LBP describes a unique encoding of the central pixel with position  $c$  regarding to its local pixel neighborhood (number of neighbors  $P$ ) using a predefined radius value  $R$ . The LBP is calculated by Eq. 1, where  $g(\cdot)$  is a gray-scale value of pixel,  $g(\cdot) \in [0 \dots 255]$ .

$$LBP_{P,R} = \sum_{p=0}^{P-1} s(g_p - g_c) 2^p, \quad \text{where } s(\cdot) = \begin{cases} 1, & s(\cdot) \geq 0 \\ 0, & s(\cdot) < 0 \end{cases} \quad (1)$$

A uniformity measure  $U$  returns the number of bitwise 0/1 and 1/0 transitions in the LBP. The LBP means the uniform LBP if  $U \leq 2$ . The 58 possible uniform patterns in  $(8, R)$  neighborhood one can find in research<sup>27</sup>. The LBPs are the gray-scale invariant because only the sign of the gray-value difference is considered. In order to extract the neighbor's gray values, the rotation-invariant variance measure  $VAR$  was introduced by Ojala et al.<sup>3</sup>:

$$VAR_{P,R} = \frac{1}{P} \sum_{p=0}^{P-1} (g_p - \mu)^2, \quad \text{where } \mu = \frac{1}{P} \sum_{p=0}^{P-1} g_p. \quad (2)$$

These two measures  $LBP_{P,R}$  and  $VAR_{P,R}$  might be used for texture classification. As Teutsch and Beyerer mentioned<sup>13</sup>, the gradient magnitude can be estimated using these parameters in a following manner:

$$G(LBP_{P,R}) = \begin{cases} \sum_{r=R_1}^{R_n} \sqrt{VAR_{P,r}}, & \text{if } LBP_{P,R} \text{ is uniform,} \\ 0, & \text{else.} \end{cases} \quad (3)$$

Also, it is possible to analyze eight different positions if a uniform LBP is not a spot (Fig. 1).

Liu et al.<sup>28</sup> proposed four LBP-like descriptors: two local intensity-based CI-LBP and NI-LBP relative to the central and neighborhood pixels, respectively, and two local difference-based descriptors RD-LBP and AD-LBP as the radial differences and angular differences, respectively. Thus, CI-LBP and NI-LBP are computed by Eq. 4.

$$CI-LBP = s(g_c - \mu_R), \quad NI-LBP_{P,R} = \sum_{p=0}^{P-1} s(g_p - \mu) 2^p, \quad \text{where } s(\cdot) = \begin{cases} 1, & s(\cdot) \geq 0 \\ 0, & s(\cdot) < 0 \end{cases} \quad (4)$$

The NI-LBP is interesting due to its property to preserve the weak edge patterns.

#### 4. Fractal properties of texture

Fractal theory based on the geometry and dimension theories describes the mathematical sets with a high degree of geometrical complexity. The images and video sequences representing the natural objects with textural surfaces involves into such mathematical sets. The self-similarity and irregularity of natural textures as the main properties are well defined by their fractal dimensions. Additional parameter is a lacunarity, which reflects a property of texture fullness because the textures with different structures may have the identical values of fractal dimension. The main approaches for estimation of these two parameters are considered in Sections 4.1 and 4.2, respectively.

##### 4.1. Fractal descriptors

The intrinsic self-similarity property of fractal objects is highlighted by the relation of fractal dimension. For images with ideal fractal structure, the fractal dimension  $D$  is computed in a view of Eq. 5, where parameters  $r$  and  $N_r$  are estimated in dependence of the chosen method.

$$D = \lim_{r \rightarrow 0} \frac{\log(N_r)}{\log(1/r)} \quad (5)$$

However, it is difficult to compute  $D$  using Eq. 1 directly. Also, the most texture images are not the ideal fractal images<sup>29</sup>. Some approximation methods were proposed in 1990s, for example, the reticular cell counting approach<sup>30</sup> and the probability modification<sup>31</sup>. From a great variety of proposed methods, the BCD method is widely employed<sup>32</sup>. More, it can be applied to the patterns with and without self-similarity.

In this case, an image with resolution  $M \times M$  pixels can be considered as a 3D surface with  $(x, y)$  projection on an image plane, where the coordinate  $z$  denoted a gray level. An image is divided into boxes with  $s \times s \times s'$  pixels, where  $s'$  is a height of each box,  $1 < s < M/2$  and  $s$  is an integer. The parameter  $r$  is defined as  $r = s/M$ . These boxes are indexed with  $(i, j)$  in the 2D space. If the minimum and maximum grayscale levels in the  $(i, j)$ th grid fall into the  $k$ th and  $l$ th boxes, respectively, then the contribution of  $n_r$  in the  $(i, j)$ th grid is defined by simple counting:

$$n_r(i, j) = l - k + 1. \tag{6}$$

The parameter  $N_r$  shows the contributions on  $n_r(i, j)$  as their summation:

$$N_r = \sum_{i,j} n_r(i, j). \tag{7}$$

The parameter  $N_r$  can be computed for different sizes of the partitioned boxes  $r$  in order to be convinced in the fractal properties of the test texture. However, if a texture image is noisy, then the fractal dimension can be estimated from the least-square linear fit of  $\log(N_r)/\log(1/r)$  using different values of parameter  $r$ .

Note that additionally other fractal measures are used in practice, for example, based on the volumetric Bouligand–Minkowski dimension and modified fractal signature called as blanket technique<sup>33</sup>. Also, it is interesting that Casanova et al.<sup>34</sup> estimated the fractal properties of texture considering a color distribution under influence of each color area on a neighborhood and without separating the image into the R, G and B channels. The final descriptor included a concatenation of all three R, G, B distributions and provided a specific representation for texture classification. However, the color textural images depend not only from the textural surface and its albedo but also from the illumination conditions and the camera viewing position and parameters of shooting.

#### 4.2. Lacunarity

Fractal dimension measures a space occupation but not how this space is occupied. This leads to the situation, when different textures have the same fractal dimension. To solve this problem, a special term called lacunarity as a special distribution of specific gap size  $l$  along the texture was introduced<sup>35</sup>. Unlike the fractal dimension, a lacunarity is a scale dependent measure. The earlier algorithms computed the lacunarity for binary textures based on the analysis of the mass distribution in a deterministic or a random set using the gliding-box approach. Hereinafter, the approach was extended for the gray-scale images. One of the most famous and simple algorithm is based on the Differential Box Counting (DBC) method proposed by Du and Yeo<sup>36</sup>. For each  $l \times l$  gliding box, the relative height of a column  $h_i(i, j)$  is calculated by Eq. 8, where  $i$  and  $j$  are the image coordinates,  $v$  and  $u$  are the maximum and minimum pixel values inside this box, respectively.

$$h_i(i, j) = \lceil v/l \rceil - \lfloor u/l \rfloor \tag{8}$$

Then the probability distribution  $P(H, l)$  is assumed by Eq. 9, where  $H$  is each relative height,  $\delta(\cdot)$  is a Kronecker's delta.

$$P(H, l) = \sum_{i,j} \delta(h_i(i, j), H) \quad \delta(x, y) = \begin{cases} 1, & x = y \\ 0, & x \neq y \end{cases} \tag{9}$$

The probability dense function  $Q(H, l)$  and, finally, the lacunarity  $\Lambda(l)$  for a box size  $l$  are defined by Eqs. 10–11, respectively.

$$Q(H, l) = P(H, l) / \sum_{\forall H} P(H, l) \quad (10)$$

$$\Lambda(l) = \sum H^2 \cdot Q(H, l) / (\sum H \cdot Q(H, l))^2 \quad (11)$$

Note that a low value of lacunarity indicates the homogeneity, while a high value of lacunarity specifies the heterogeneity structure of texture. The approach, when a lacunarity is computed in terms of the local binary patterns, was proposed by Backes<sup>37</sup>. This approach is based on the gliding-box method designed for binary and the DBC method for gray scale images. Backes computed the mass as a sum of 1 in the LBP operator. The obtained results demonstrated the computational simplicity and accuracy.

## 5. Recommendations for region choice

The goal of preprocessing is to choose the preferable regions for embedding. The following recommendations can be applied in still image watermarking:

- Use the LBP modifications like extended LBP or NI-LBP in time-consuming and memory-consuming applications, for example, mobile devices.
- Use fractal descriptors as more accurate approach to estimate a degree of texturing in some cases.
- Try to estimate a degree of texturing, such as high, middle, and low textured regions for a non-proportional embedding of the watermark bits.
- Evaluate the color, illumination and contrast properties of a watermark and select the regions with similar parameters in a host image.
- Apply regions with blue tone for embedding because they possess lesser sensitivity for a human vision.

As a result, an embedding mask may be created and transmitted as a part of a secret key or the same algorithm for the regions' choice might be applied to the watermarked image during extraction stage. Examples of preferable texture areas for a watermarking based on the textural segmentation are depicted in Fig. 2.



Fig. 2. examples of preferable texture areas for watermarking: dark green – high disable, light green – low disable.

Such recommendations cannot be considered as the strong ones. However, in some cases they may be useful.









## 6. Experimental results

For experiments, five categories of images with total number 9,259 images from Ponce Group Dataset<sup>38</sup> were used:

- Category “Birds” contains 600 images of six different classes of birds (with 100 samples in each class), such as Egret, Mandarin duck, Snowy owl, Puffin, Toucan, and Wood duck
- Category “Butterflies” includes 619 images of seven different classes of butterflies, such as Admiral (111 images), Black Swallowtail (42 images), Machaon (83 images), Monarch 1 (wings closed) (74 images), Monarch 2 (wings open) (84 images), Peacock (134 images), and Zebra (91 images)
- Category “Coil-100” involves 7,200 studio shooting images with close-up salient objects like cups, vegetables, fruits, toys, etc.
- Category “Copydays original” comprises 157 images of nature, humans, and animals
- Category “Scene categories” keeps 683 images of three different classes, such as Industrial scenes (226 images), Bedroom photos (216 images), and CAL suburb (241 images)

These images have different resolution with minimum values  $128 \times 128$  pixels and maximum values  $2048 \times 1536$  pixels and depict a great variety of objects, including natural objects, man-made objects, humans, animals, etc., under the outdoor and indoor shooting. Some examples of the used images are described shortly in Table 1.

Table 1. Description of some used images.

| Description of test image   | Sample image  | Description of test image  | Sample image  |
|---|---|--|---|
| File name: coil-100\coil-100\obj45_0.png<br>Resolution, pixels: $128 \times 128$<br>Alias: image1         |   | File name: scene_categories\industrial\image_0001.jpg<br>Resolution, pixels: $220 \times 247$<br>Alias: image2 |   |
| File name: birds\puffin\puf004.jpg<br>Resolution, pixels: $238 \times 211$<br>Alias: image3               |  | File name: birds\puffin\wod096.jpg<br>Resolution, pixels: $640 \times 480$<br>Alias: image4                    |  |
| File name: butterflies\monarch_closed\mnc058.jpg<br>Resolution, pixels: $700 \times 596$<br>Alias: image5 |  | File name: copydays_original\204900.jpg<br>Resolution, pixels: $1600 \times 1200$<br>Alias: image6             |  |
| File name: copydays_original\200100.jpg<br>Resolution, pixels: $2048 \times 1536$<br>Alias: image7        |  | File name: copydays_original\206300.jpg<br>Resolution, pixels: $2048 \times 1536$<br>Alias: image8             |  |



The example of an original image, two fragments (homogeneity and textural), and their histograms built by use of the LBP technique are depicted in Fig. 3.

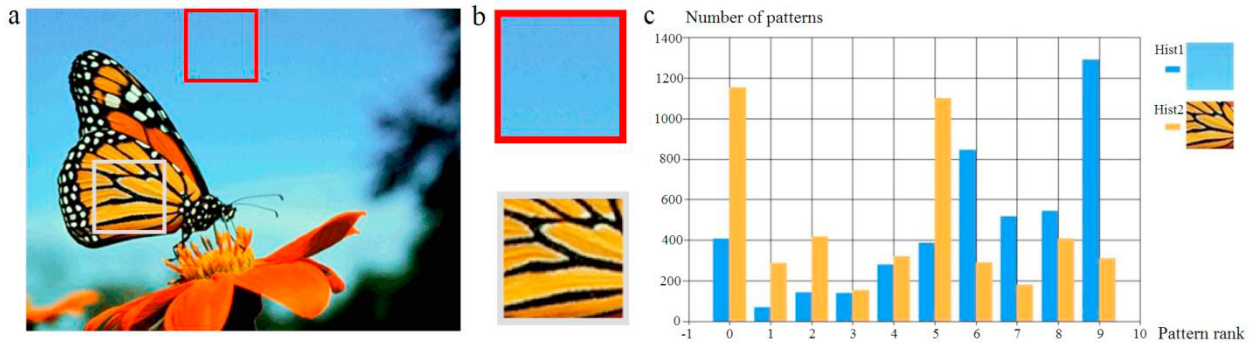


Fig. 3. (a) original image; (b) its fragments; (c) histograms of fragments.

The example of a high textural area segmented by fractal technique is depicted in Fig. 4.



Fig. 4. high textural area segmented by fractal technique.

The comparative results for detection of high textural areas in images using the LBPs and fractal techniques are given in Table 2. The output results of the designed software tool were compared with the expert results of high textural areas in images segmented manually. The expert evaluations were accepted as 100%. A parameter of textural area TA provided by the software tool is the estimation regarding to expert evaluation. False Rejection Rate (FRR) shows a number of missing pixels in the high textural areas, while False Acceptance Rate (FAR) calculates a number of pixels acceptable as the pixels of the high textural areas.

Table 2. The comparative results of detection of high textural areas in images, representing in Table 1.

| Test image | LBP technique |        |        | Fractal technique |        |        |
|------------|---------------|--------|--------|-------------------|--------|--------|
|            | TA, %         | FRR, % | FAR, % | TA, %             | FRR, % | FAR, % |
| Image1     | 100.0         | 0.00   | 0.00   | 100.0             | 0.00   | 0.00   |
| Image 2    | 106.7         | 6.41   | 4.11   | 108.2             | 1.54   | 5.10   |
| Image3     | 100.4         | 0.11   | 0.98   | 100.6             | 0.78   | 1.00   |
| Image4     | 98.63         | 2.01   | 7.00   | 99.12             | 3.00   | 9.10   |
| Image5     | 101.3         | 1.74   | 3.41   | 99.54             | 1.14   | 4.00   |
| Image6     | 100.0         | 0.00   | 0.00   | 100.16            | 0.21   | 0.09   |
| Image7     | 96.28         | 4.32   | 4.12   | 97.41             | 4.00   | 3.99   |
| Image8     | 97.74         | 3.14   | 6.41   | 96.41             | 4.10   | 7.01   |



The comparative estimations for running times of two techniques based on the fractals and the LBP computation are placed in Table 3. Values of running time were obtained using a laptop Lenovo Intel Core i5-3230m CPU 2.60 GHz, RAM 4.00 GB under operating system Windows 7. As it seems from Table 3, the running time depends from an image resolution strongly. A parameter of textural area shows a share in percentages of textural area regarding to the whole image area.

Table 3. Computational time of the LBP and fractal techniques implementation.

| Test image | Resolution, pixels | Textural area, % | Running time, ms (fractal) | Running time, ms (LBP) |
|------------|--------------------|------------------|----------------------------|------------------------|
| Image1     | 128×128            | 5.45             | 130                        | 67.8                   |
| Image2     | 220×247            | 62.9             | 200                        | 89.8                   |
| Image3     | 238×211            | 72.7             | 198                        | 97.2                   |
| Image4     | 640×480            | 100              | 274                        | 135                    |
| Image5     | 700×596            | 86.2             | 243                        | 142                    |
| Image6     | 1600×1200          | 84.5             | 351                        | 174                    |
| Image7     | 2048×1536          | 94.4             | 641                        | 312                    |
| Image8     | 2048×1536          | 91.7             | 701                        | 312                    |

The experimental results demonstrate that an average processing time of algorithm based on the LBP technique exceeds in one and a half times an average processing time of algorithm based on the fractal technique, while the evaluations of the segmented textural areas are close. Therefore, the LBP technique used in preliminary textural analysis (before embedding/extraction stages of a watermark) can be recommended for the mobile applications.

## 7. Conclusions

In the most cases, the efficiency of embedding/extraction of a watermark from a still image depends from the applied watermarking method and detection of preferable areas for embedding. In this study, it was shown that the textural analysis helps to detect such preferable areas. Two methods based on the fractal descriptors and the LBP modifications were tested. The obtained experimental results demonstrated close values in textural area detection and significant differences in time consuming. The application of the LBP modifications is reasonable in mobile applications with the restricted computational sources. In future, the influence of different attacks on the selection of preferable for watermarking areas in the images and video sequences will be investigated.

## References

1. Bianchi T. Secure watermarking for multimedia content protection: a review of its benefits and open issues. *IEEE Sig Process Magaz* 2013;**30**(2):87-96.
2. Zhang J, Marszalek M, Lazebnik S, Schmid C. Local features and kernels for classification of texture and object categories: A comprehensive study. *Int J Comput Vis* 2007;**73**(2):213-238.
3. Ojala T, Pietikäinen M, Mäenpää T. Multiresolution gray-scale and rotation invariant texture classification with local binary patterns. *IEEE Trans Pattern Anal Mach Intell* 2002;**24**(7):971-987.
4. Liu L, Fieguth P. Texture classification from random features. *IEEE Trans Pattern Anal Mach Intell* 2012;**34**(3):574-586.
5. Sandler R, Lindenbaum M. Optimizing Gabor filter design for texture edge detection and classification. *Int J Comput Vis* 2009;**84**(3):308-324.
6. Xu Y, Ji H, Fermüller C. Viewpoint invariant texture description using fractal analysis. *Int J Comput Vis* 2009;**83**(1):85-100.
7. de Mesquita SáJunior JJ, Backes AR, Cortez PC. Texture analysis and classification using shortest paths in graphs. *Pattern Recognit Lett* 2013;**34**(11):1314-1319.
8. Rivera AR, Chae O. Spatiotemporal directional number transitional graph for dynamic texture recognition. *IEEE Trans Pattern Anal Mach Intell* 2015;**37**(10):2146-2152.
9. Backes AR, Bruno OM. Plant leaf identification using multi-scale fractal dimension. In: Foggia P, Sansone C, Vento M, editors. *Image Analysis and Processing – ICAP 2009*, Springer, Berlin, Heidelberg; 2009. LNCS, vol. 5716, p. 143-150.
10. Varma M, Garg R. Locally invariant fractal features for statistical texture classification. International Conference on Computer Vision 2007, Rio de Janeiro, Brazil, 1-8.

11. Ojala T, Pietikäinen M, Harwood D. A comparative study of texture measures with classification based on featured distributions. *Pattern Recognit* 1996;**29**(1):51-59.
12. Zhou H, Wang R, Wang C. A novel extended local-binary-pattern operator for texture analysis. *Information Sciences* 2008;**178**(22):4314-4325.
13. Teutsch M, Beyerer J. Noise resistant gradient calculation and edge detection using local binary patterns. In: Park JI, Kim J, editors. *Computer Vision - ACCV 2012 Workshops*. Springer, Berlin, Heidelberg; 2013. LNCS, vol. 7728, p. 1-14.
14. Yang H, Wang Y. A LBP-based face recognition method with Hamming distance constraint. International Conference on Image and Graphics 2007, Chengdu, Sichuan, China, 645-649.
15. Liao S, Law MWK, Chung ACS. Dominant local binary patterns for texture classification. *IEEE Trans Image Proc* 2009;**18**(5):1107-1118.
16. Huang X, Li SZ, Wang Y. Shape localization based on statistical method using extended local binary pattern. International Conference on Image and Graphics 2004, Hong Kong, China, 184-187.
17. Zhao S, Gao Y, Zhang B. Sobel-LBP. International Conference on Image Processing 2008, San Diego, California, USA, 2144-2147.
18. Mandelbrot BB, Van Ness JW. Fractional Brownian motions, fractional noises and applications. *SIAM Rev* 1968;**10**:422-437.
19. Jin XC, Ong SH, Jayasooriah. A practical method for estimating fractal dimension. *Pattern Recognit Lett* 1995;**16**(5):457-464.
20. Asvestas P, Matsopoulos GK, Nikita KS. Estimation of fractal dimension of images using a fixed mass approach. *Pattern Recognit Lett* 1999;**20**(3):347-354.
21. Mattila P. *Geometry of sets and measures in euclidean spaces: fractals and rectifiability*. Cambridge: Cambridge University Press; 1995
22. Li J, Du Q, Sun C. An improved box-counting method for image fractal dimension estimation. *Pattern Recognit* 2009;**42**(11):2460-2469.
23. Manoel ETM, da Fontoura Costa L, Streicher J, Müller GB. Multiscale fractal characterization of three-dimensional gene expression data. Fifteenth Brazilian Symposium on Computer Graphics and Image Processing 2002, Fortaleza-CE, Brazil, 269-274.
24. Lazebnik S, Schmid C, Ponce J. A sparse texture representation using affine-invariant regions. *IEEE Trans Pattern Anal Mach Intell* 2005;**8**(27):1265-1278
25. Barreira L, Pesin, Y Schmeling J. On a general concept of multifractality: Multifractal spectra for dimensions, entropies, and Lyapunov exponents. Multifractal rigidity. *Chaos* 1997;**7**(1):27-38.
26. Xu Y, Yang X, Ling H, Ji H. A new texture descriptor using multifractal analysis in multi-orientation wavelet pyramid. IEEE Conference on Computer Vision and Pattern Recognition 2010, San Francisco, USA, 161-168.
27. Pietikäinen M, Hadid A, Zhao G, Ahonen T. Local binary patterns for still images. In: Pietikäinen M, Hadid A, Zhao G, Ahonen T, editors. *Computer Vision Using Local Binary Patterns*, Springer-Verlag London Limited. 2011, p. 13-47.
28. Liu L, Zhao L, Long Y, Kuang G, Fieguth P. Extended local binary patterns for texture classification. *Image and Vision Computing* 2012;**30**(2):86-99.
29. Favorskaya M, Petukhov N. Comprehensive calculation of the characteristics of landscape images. *J Optical Technology* 2010;**77**(8):504-509.
30. Gangepain JJ, Roques-Carnes C. Fractal approach to two dimensional and three dimensional surface roughness. *Wear* 1986;**109**:119-126.
31. Keller J, Crownover R, Chen S. Texture description and segmentation through fractal geometry. *Comput Vision Graphics Image Process* 1989;**45**:150-160.
32. Peitgen HO, Jurgens H, Saupe D. *Chaos and fractals new frontiers of science*. 2nd ed. New York: Springer-Verlag; 2004.
33. Peleg S, Naor J, Hartley R, Avnir D. Multiple resolution texture analysis and classification. *IEEE Trans Pattern Anal Mach Intell* 1984;**6**(4):518-523.
34. Casanova D, Florindo JB, Falvo M, Bruno OM. Texture analysis using fractal descriptors estimated by the mutual interference of color channels. *Information Sciences* 2016;**346-347**:58-72.
35. Mandelbrot B. *The fractal geometry of nature*. New York, WH Freeman and Company, 1982.
36. Du G, Yeo TS. A novel lacunarity estimation method applied to SAR image segmentation. *IEEE Trans Geoscience Remote Sens* 2002;**40**(12):2687-2691.
37. Backes AR. A new approach to estimate lacunarity of texture images. *Pattern Recognit Lett* 2013;**34**(13):1455-1461.
38. Datasets for Computer Vision Research. Available at: [http://www-cvr.ai.uiuc.edu/ponce\\_grp/data/](http://www-cvr.ai.uiuc.edu/ponce_grp/data/)